

New developments in energy transfer and transport studies in relativistic laser–plasma interactions

This article has been downloaded from IOPscience. Please scroll down to see the full text article.

2010 Plasma Phys. Control. Fusion 52 124046

(<http://iopscience.iop.org/0741-3335/52/12/124046>)

View [the table of contents for this issue](#), or go to the [journal homepage](#) for more

Download details:

IP Address: 130.183.90.175

The article was downloaded on 04/01/2011 at 10:43

Please note that [terms and conditions apply](#).

New developments in energy transfer and transport studies in relativistic laser–plasma interactions

P A Norreys^{1,2}, J S Green¹, K L Lancaster¹, A P L Robinson¹,
R H H Scott^{1,2}, F Perez³, H-P Schlenvoigt³, S Baton³, S Hulin⁴,
B Vauzour⁴, J J Santos⁴, D J Adams⁵, K Markey⁵, B Ramakrishna⁵,
M Zepf⁵, M N Quinn⁶, X H Yuan⁶, P McKenna⁶, J Schreiber^{2,7},
J R Davies⁸, D P Higginson^{9,10}, F N Beg⁹, C Chen¹⁰, T Ma¹⁰ and P Patel¹⁰

¹ Central Laser Facility, STFC Rutherford Appleton Laboratory, Harwell Science and Innovation Campus, Didcot, Oxon OX11 0QX, UK

² Blackett Laboratory, Imperial College London, Prince Consort Road, London SW7 2BZ, UK

³ Laboratoire pour l'Utilisation des Lasers Intenses, École Polytechnique, route de Saclay, 91128 Palaiseau Cedex, France

⁴ Centre Lasers Intenses et Applications, Université Bordeaux 1-CNRS-CEA, Talence, France

⁵ School of Mathematics and Physics, Queens University Belfast, Belfast BT7 1NN, UK

⁶ Department of Physics, University of Strathclyde, John Anderson Building, 107 Rottenrow, Glasgow G4 0NG, UK

⁷ Max-Planck-Institut für Quantenoptik, Hans-Kopfermann-Str. 1, D-85748 Garching, Germany

⁸ Grupo de Lasers e Plasmas, Instituto Superior Técnico, Av. Rovisco Pais, 1049-001, Lisbon, Portugal

⁹ Department of Mechanical and Aerospace Engineering, University of California, San Diego 9500 Gilman Dr., La Jolla, CA 92093, USA

¹⁰ Lawrence Livermore National Laboratory, 7000 East Avenue, Livermore, CA 94550, USA

Received 16 July 2010, in final form 23 September 2010

Published 15 November 2010

Online at stacks.iop.org/PPCF/52/124046

Abstract

Two critical issues related to the success of fast ignition inertial fusion have been vigorously investigated in a co-ordinated campaign in the European Union and the United States. These are the divergence of the fast electron beam generated in intense, PW laser–plasma interactions and the fast electron energy transport with the use of high intensity contrast ratio laser pulses. Proof is presented that resistivity gradient-induced magnetic fields can guide fast electrons over significant distances in (initially) cold metallic targets. Comparison of experiments undertaken in both France and the United States suggests that an important factor in obtaining efficient coupling into dense plasma is the irradiation with high intensity contrast ratio laser pulses, rather than the colour of the laser pulse itself.

(Some figures in this article are in colour only in the electronic version)

1. Introduction

The concept of fast ignition inertial fusion [1] involves the separation of the compression of deuterium–tritium fusion fuel to ultra-high density and the heating of a small off-centre hot spot region at peak compression by energy deposition of copious numbers of megaelectronvolt electrons (that are generated in intense laser–plasma interactions). The range of the relativistic electrons in the dense compressed fuel is similar to that of 3.5 MeV $d(t,n)^4\text{He}$ fusion alpha-particles. The hot spot formation occurs on a timescale short enough that the plasma does not have time to respond by hydrodynamic motion. The scheme has attracted a great deal of interest and attention since its invention for two reasons. Firstly, the symmetry requirements for the compression of the fuel to ultra-high density are significantly relaxed. This is due to the lower implosion velocity and the reduced target aspect ratio, which act to mitigate the deleterious growth of the Rayleigh–Taylor hydrodynamic instability. Secondly, more fuel can be compressed with lower compression drive energies, potentially leading to higher fusion energy gain compared with conventional central hot spot schemes for inertial confinement fusion [2].

The success of cone-guided fast ignition has two vital ingredients [3]. The first is that the energy needed to heat the hot spot region to ignition temperatures is minimized. This clearly impacts the scale of the petawatt laser facility required to ignite the fusion pellet at peak compression. Above all, it demands that the divergence of the fast electron beam, generated in the intense laser–plasma interaction, is controlled [4–6]. The divergence has been found to depend upon two factors: firstly, rippling of the density of the critical surface on the scale of the laser wavelength (in addition to larger scale hole boring) which is important for plasmas with a relatively large density scale length [7–9]; secondly, deflections from magnetic fields generated by the filamentation instability as the fast electrons enter the target [10–12]. In this context, it is interesting to note that an intensity dependence to the beam divergence has been identified from the reported literature and measurements with fast ignition relevant intensities and pulse durations [4], reaching over 50° at the highest intensities reported [13]. Those observations were supported by matching particle-in-cell simulations of the interaction.

A promising solution to the divergence problem is to generate sufficiently large magnetic fields in overdense plasma such that the fast electrons are pinched on-axis and the energy transport is collimated [14]. In recent petawatt laser–solid interaction experiments, resistivity-gradient generated magnetic collimation has been shown to restrict energy flow in one plane by the use of structured target that comprised a high resistivity layer (Sn) sandwiched between two layers of lower resistivity material (Al) [15] in a Queens University Belfast-led collaboration involving the Rutherford Appleton Laboratory/Imperial College London and the University of Strathclyde. In the work reported in section 2, magnetic collimation has been extended to radial confinement and axial guiding by the use of a high resistivity wire target (in this case, Fe) embedded in a low resistivity material (Al), by the same team [16].

The second vital ingredient for fast ignition success is that, at the same time as the energy needed to form the hot spark is minimized, the energy coupling to the overdense plasma is maximized. This requires a revisit to the fundamental understanding of both energy absorption and coupling in strongly relativistic laser–solid interactions. This is especially important for small scale-length laser–solid density target interactions, now that it has been established that energy coupling is reduced with larger scale-length plasmas generated in cone targets [17, 18] and improved intensity contrast ratio pulses are now required.

In section 3, results from both ω_0 and $2\omega_0$ experiments conducted on the pico2000 facility at LULI, Ecole Polytechnique are briefly described and compared with data obtained on the Titan and Trident laser facilities. A summary of the findings is presented in section 4.

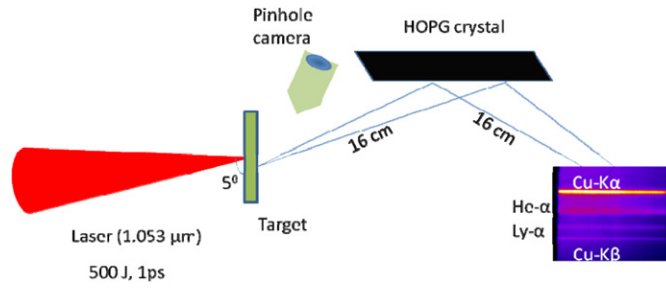


Figure 1. Schematic illustration of the experimental arrangement of diagnostics which looked at Cu K_{α} emission from a $15 \mu\text{m}$ thick layer located at the rear surface of the target. The Cu K_{α} pinhole cameras were at 20° and 50° to the horizontal and vertical target normal axis. The HOPG diagnostic was placed 13° to the target normal for the measurement of Cu K_{α} lines. The resistivity gradient targets had an iron core of either 25 or $50 \mu\text{m}$ diameter surrounded by a $250 \mu\text{m}$ diameter Al cladding, with variable length.

2. Resistivity gradient magnetic collimation

The concept of resistivity gradient-induced collimation follows from a combination of Faraday's and Ohm's laws:

$$\frac{\partial \underline{B}}{\partial t} = \eta \nabla \times \underline{j} + (\nabla \eta) \times \underline{j}, \quad (1)$$

where \underline{j} is the fast electron current and η is the plasma resistivity. The first term in equation (1) generates a \underline{B} -field that acts to push electrons into regions of higher current density and causes focusing, pinching and collimation of the beam. It can also lead to beam filamentation. The second term in equation (1) indicates that the B -field will grow at resistivity gradients such that fast electrons are pushed into regions of higher resistivity. In unstructured targets, the first term dominates initially. As the temperature rises, the resistivity falls faster than linearly with temperature and the magnetic field eventually changes sign and hollows rather than focuses the beam [19, 20]. Extensive computational modelling by Robinson and Sherlock [14] confirmed that by suitable structuring of the target with materials of different resistivity, the second term can be utilized to guide the fast electrons into the region of higher resistivity. The first proof-of-concept experiment involved the use of structured target that comprised a high resistivity layer (Sn) sandwiched between two layers of lower resistivity material (Al). Evidence has been presented that the fast electron energy deposition is restricted to flow in the high resistivity plane [15].

The proof-of-principle experiment has now been extended to two dimensions with the use of an embedded high resistivity wire target in lower resistivity material [16]. The experiment was performed at Rutherford Appleton Laboratory employing the VULCAN petawatt laser system. After reflection from a plasma mirror, the 1054 nm laser pulse delivered 150 J of energy on target in a pulse in the range $0.5\text{--}0.8 \text{ ps}$ full width at half maximum (FWHM) duration. The p-polarized laser pulse was focused to a peak intensity of up to $\sim 10^{20} \text{ W cm}^{-2}$ on target at 5° angle of incidence. The focal spot is characterized by a q -Gaussian spatial profile given by $[1 + (r/4.45 \mu\text{m})^2]^{-1.47}$ where 50% of the incident laser energy is encircled within a diameter of $16 \mu\text{m}$, the remaining energy extended out to $50 \mu\text{m}$ [21, 22].

The primary diagnostic of the collimation effect was provided by Cu K_{α} radiation emitted from a $15 \mu\text{m}$ Cu tracer layer at the rear side of the targets. A schematic illustration of the experiment is shown in figure 1. The size of the emitting region from the Cu layer was diagnosed using an x-ray pinhole camera, a spherical quartz crystal imager and source broadening with a

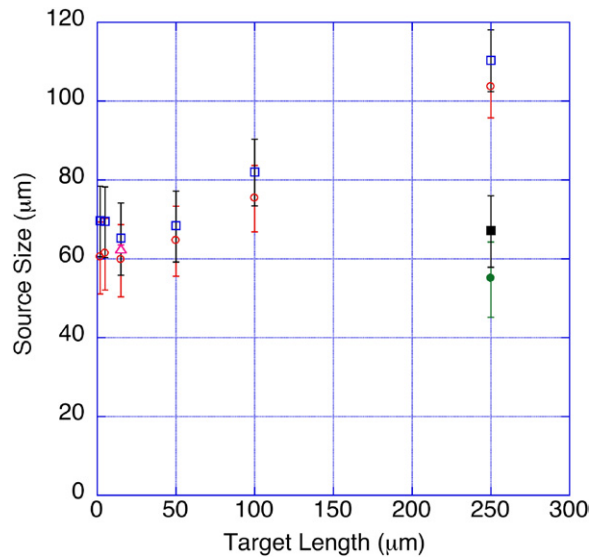


Figure 2. Plotted here is the x-ray spot size FWHM for uniform targets (open symbols) and guiding-targets (full symbols) against target length. Measurements with the crystal imager are shown as triangles, x-ray pinhole camera as circles while HOPG data are shown as squares. The effect of collimation is clearly visible at 250 μm target thickness resulting in near resolution limited source sizes. The data points represent an average over the data set for each thickness for clarity with the collimation data set taken over four shots. The uncertainties are calculated based on the measurement error in the x-ray spot size.

highly ordered pyrolytic graphite (HOPG) spectrometer. The pinhole camera had four 50 μm pinholes which were filtered to select different spectral ranges in the range of 1.7 to >10 keV. Image plates were used as the detectors. The HOPG crystal spectrometer provided data on the relative K_{α} yield of the targets as well as an independent measure of the source size due to the source broadening of the measured line-width.

On the one hand, the x-ray emission size from the guided target was similar to the pinhole size, thereby limiting the spatial resolution obtained. On the other hand, the agreement, within the experimental error, between the source size obtained by the two diagnostics demonstrates that the HOPG source broadening is indeed a good way to measure the x-ray source size and that source broadening dominates the measured line-width under these conditions. The full data set therefore allows a direct comparison of the divergence of the fast electron beam both with and without the guiding wire under identical irradiation conditions.

Figure 2 shows the FWHM of the data obtained with both uniform and structured collimator targets. The uniform reference targets show a divergence angle of 27° FWHM, somewhat smaller than that measured by Lancaster *et al* [13] and by Green *et al* [4] for similar intensities (50°). One explanation is that the difference is the use of the plasma mirror in this experiment. The plasma mirror has the effect of improving the intensity contrast ratio of the main interaction pulse with its pedestal, thereby reducing the size and scale length of the preformed plasma and, with that, the rippling of the critical surface, hole boring and micro-channel formation during the main interaction pulse. The important point to note is that the structured target shows identical spot size to that measured in the thinnest reference targets (65 μm). The relative K_{α} signal is $\sim \times 2$ higher in the guided target, compared with a reference Fe iron target (measured at 250 μm total target thickness). The measurements confirm the resistivity

induced magnetic guiding of the fast electrons. Supporting 3D simulations will be reported shortly in [16].

3. Energy transport studies comparing ω_0 and $2\omega_0$ light

Studies of energy absorption and transport comparing both fundamental and second harmonic laser irradiation of laser–plasma interaction at relativistic intensities are essential. Frequency conversion is attractive in that it allows greater control over the intensity contrast ratio. Every intense laser pulse had a pedestal associated with the main picosecond interaction pulse. This pedestal arises from a combination of amplified spontaneous emission (ASE) and residual dispersion from imperfect recompression of the amplified stretched pulse. The wide range of energy levels available in the different laser facilities allows comparison of energy coupling with a wide range of density scale-length interactions, ranging from sharp vacuum–solid density interface interactions at the cone tip (because the intensity of the pedestal pulse is below the breakdown threshold of the solid material) to those with relatively large scale lengths ($L > 10 \mu\text{m}$) [23]. In addition, Wei *et al* have shown that, in large scale-length conditions, self-generated magnetic fields arise between the critical density surface and the overdense region, preventing the entry of fast electrons into the solid density target. This bottleneck effect is removed with improved intensity contrast ratio pulses [23]. An additional benefit to frequency conversion is that it reduces the fast electron temperature due to the lower value of ponderomotive potential of the laser pulse for the same intensity on target, which is desirable for fast ignition [1].

The experiments were performed using three different laser facilities. The first was the pico2000 facility at the LULI laboratory, École Polytechnique. This laser delivered pulses of 1053 nm/1 ps in one experiment. The laser energy in each pulse was in the range 35–45 J with an average irradiance on target of $I\lambda^2 \sim 2 \times 10^{19} \text{ W cm}^{-2} \mu\text{m}^2$. The pre-pulse had an energy measured to be 100 mJ in 3 ns, providing an intensity contrast ratio of $\sim 1 : 10^{-6}$ between the peak intensity and that of the pedestal. In a second experiment, the pulse was frequency doubled and delivered 527 nm/1 ps pulses with energies between 7 and 30 J, providing irradiances on target with $I\lambda^2$ of $(1\text{--}4) \times 10^{18} \text{ W cm}^{-2} \mu\text{m}^2$. The use of three dielectric coated mirrors for 527 nm radiation reduced the pedestal energy to $< 10 \mu\text{J}$ energy and provided a $\sim 1 : 10^{-10}$ intensity contrast ratio.

The second laser facility was the Titan laser at Lawrence Livermore National Laboratory (1053 nm/0.7–1.0 ps). The laser energy was varied from 15 to 150 J and provided pulses with $I\lambda^2$ between 2×10^{19} – $2 \times 10^{20} \text{ W cm}^{-2} \mu\text{m}^2$. The pedestal was in the range 10–100 mJ. The facility also allowed nanosecond duration pulses with variable energy to be injected before the main picosecond pulse arrived [18, 19].

The third laser facility used was the Trident laser facility in Los Alamos National Laboratory (1053 nm/1 ps). The laser energy was varied between 20 and 75 J and generated pulses with $I\lambda^2$ between 2×10^{18} – $2 \times 10^{19} \text{ W cm}^{-2} \mu\text{m}^2$. The laser had a measured pedestal of $< 1 \mu\text{J}$ an intensity contrast ratio of $\sim 1 : 10^{-11}$.

The essential features of the experimental results are the following.

Firstly, line-fitting of $K_{\alpha-1}$ and $K_{\alpha-2}$ x-ray emission spectra from buried Cu layers [24] in variable thickness planar Al foil targets suggests an increased background electron heating with $2\omega_0$ ($\sim 10^{-10}$ intensity contrast ratio) irradiation compared with ω_0 ($\sim 10^{-6}$ contrast ratio) irradiation on the LULI facility by as much as 50%. Caution is needed in this interpretation; time-resolved optical pyrometry measurements (similar to those reported by Nakatsutsumi *et al* [25]) taken at the same time as the x-ray spectroscopy show similar temperatures on the rear surface of the irradiated foil targets. The difference between the two methods is likely due

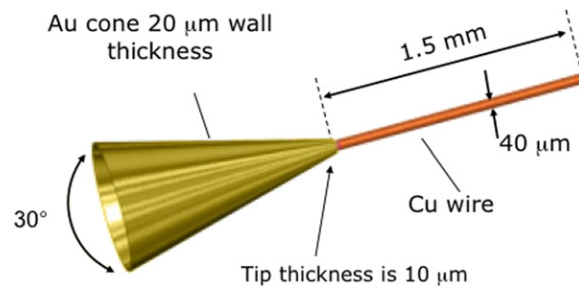


Figure 3. Schematic illustration of the targets used in the three laser facilities. The Cu K_{α} emission was measured with the use of HOPG spectrometers and absolutely calibrated image plate detectors.

to the different spatial resolution of each instrument, with different spatial regions contributing to the signals.

Secondly, the fast electron energy coupling into cone-wire targets is increased by $\times 2$ for higher contrast ratio irradiation; by comparison of the integrated K_{α} yields from identical cone-wire targets irradiated using absolutely calibrated detectors at the $2\omega_0$ LULI and ω_0 Titan facilities. The target configuration used in all three facilities is shown in figure 3. The targets were fielded by the UC San Diego / LLNL team, in collaboration with colleagues from the Rutherford Appleton Laboratory, Imperial College London, the LULI Laboratory, CELIA in the University of Bordeaux and IST Lisbon, Portugal.

Comparison of all high contrast ratio shots from the pico2000 and Trident facilities confirms that the relative K_{α} yield (normalized to laser energy on target) is similar for both ω_0 and $2\omega_0$ irradiation. The data therefore suggest that the higher contrast ratio laser pulses are responsible for reducing the density scale length of the interaction. This reduces the micro-channelling in the plasma generated at the cone tip which, in turn, allows the increased coupling and (potentially) the increased background plasma heating. The colour of the laser pulse itself does not appear to be playing a significant role. Again, caution is required here—the value of $I\lambda^2$ in the $2\omega_0$ LULI experiment is such that it is only starting to enter the relativistic intensity regime. Experiments at higher values of $I\lambda^2$ and $2\omega_0$ are planned on the TITAN facility in the near future to confirm that this result continues at higher intensities required for fast ignition.

Thirdly, the initial diameter of the x-ray spot for the $2\omega_0$ irradiation case at LULI is about half of that generated in the ω_0 irradiation case, using the same facility. Also, the typical depth of the signal from the K_{α} fluor layer is slightly larger for $2\omega_0$. This is in contrast to the ω_0 case, where the x-ray spot radius is similar to the typical depth. This implies that the electrons go preferentially in the forward direction into the target in the $2\omega_0$ case, whereas at ω_0 the electron beam is much closer to being isotropic.

4. Summary

Crucial issues related to the success of fast ignition inertial fusion have been vigorously investigated in a coordinated campaign across the European Union and the United States. Proof has been presented that resistivity gradient-induced magnetic fields can guide fast electrons over significant distances in (initially) cold metallic targets. Previous experiments undertaken in planar geometry have now been extended to the demonstration of radial confinement and axial guiding. A comparison of four experiments undertaken in France and the United States suggests that a significant factor in obtaining efficient coupling into dense plasma is the irradiation of

metallic targets with high intensity contrast ratio pulses, rather than the colour of the laser pulse itself. The reduced scale length appears to remove the effect of micro-cavitation around the critical density surface and the bottling-up of energy close to the solid density surface by self-generated magnetic fields. Caution is required here; additional $2\omega_0$ experiments at higher values of $I\lambda^2$ and high contrast ratio are needed to confirm this effect. Finally, the fast electron beam appears to be more anisotropic with $2\omega_0$ irradiation, with more forward going fast electrons than for ω_0 irradiation with poorer intensity contrast ratio, where the beam appears to be effectively isotropic. Clearly, the colour of the laser pulse itself remains a design choice for obtaining the appropriate mean energy of the fast electrons for full scale fast ignition [26].

Acknowledgments

The authors gratefully thank the staff of the Central Laser Facility, Rutherford Appleton Laboratory, the LULI Laboratory, École Polytechnique, the Titan laser facility, Lawrence Livermore National Laboratory and the Trident laser facility, Los Alamos National Laboratory for their invaluable assistance in the execution of this work. The work was partly supported by the HiPER preparatory project, the UK Science and Technology Facilities Council, the Engineering and Physical Sciences Research Council and LaserLab Europe. Parts of the work were performed under the auspices of the US Department of Energy by Lawrence Livermore National Laboratory under Contract DE-AC52-07NA27344.

References

- [1] Tabak M *et al* 1994 *Phys. Plasmas* **1** 1626
- [2] Nuckolls J H *et al* 1972 *Nature* **239** 139
- [3] Kodama R *et al* 2001 *Nature* **412** 798
- [4] Green J S *et al* 2008 *Phys. Rev. Lett.* **100** 015003
- [5] Norreys P A *et al* 2009 *Nucl. Fusion* **49** 104023
- [6] Atzeni S *et al* 2009 *Nucl. Fusion* **49** 055008
- [7] Wilks S C, Kruer W L, Tabak M and Langdon A B 1992 *Phys. Rev. Lett.* **69** 1383
- [8] Pukhov A and Meyer-ter-Vehn J 1997 *Phys. Rev. Lett.* **79** 2686
- [9] Lasinski B F *et al* 1999 *Phys. Plasmas* **6** 2041
- [10] Ren C *et al* 2004 *Phys. Rev. Lett.* **93** 185004
- [11] Adam J C, Heron A and Laval G 2006 *Phys. Rev. Lett.* **97** 205006
- [12] Silva L O *et al* 2002 *Phys. Plasmas* **9** 2458
- [13] Lancaster K L *et al* 2007 *Phys. Rev. Lett.* **98** 125002
- [14] Robinson A P L and Sherlock M 2007 *Phys. Plasmas* **14** 083105
- [15] Kar S *et al* 2009 *Phys. Rev. Lett.* **102** 055001
- [16] Ramakrishna B *et al* 2010 *Phys. Rev. Lett.* **105** 135001
- [17] Baton S *et al* 2008 *Phys. Plasmas* **15** 042706
- [18] van Woerkom L *et al* 2008 *Phys. Plasmas* **15** 056304
- [19] MacPhee A *et al* 2010 *Phys. Rev. Lett.* **104** 055002
- [20] Davies J R 2003 *Phys. Rev. E* **68** 056404
- [21] Davies J R, Green J S and Norreys P A 2006 *Plasma Phys. Control. Fusion* **48** 1181
- [22] Patel P K *et al* 2005 *Plasma Phys. Control. Fusion* **47** B833
- [23] Wei M S *et al* 2008 *Phys. Plasmas* **15** 083101
- [24] Chung H-K *et al* 2005 *High Energy Density Phys.* **1** 3–12
- [25] Nakatsutsumi M *et al* 2008 *New J. Phys.* **10** 043046
- [26] Atzeni S *et al* 2008 *Phys. Plasmas* **15** 056311